© 2014. Published by The Company of Biologists Ltd | Journal of Cell Science (2014) 127, 4279–4291 doi:10.1242/jcs.154005

RESEARCH ARTICLE

Moonlighting cell-surface GAPDH recruits apotransferrin to effect iron egress from mammalian cells

Navdeep Sheokand[1], Himanshu Malhotra[1], Santosh Kumar[1], Vikas A. Tillu[1], Anoop S. Chauhan[1], Chaaya I. Raje[2] and Manoj Raje[1,*]

ABSTRACT

Iron (Fe^{2+}, Fe^{3+}) homeostasis is a tightly regulated process, involving precise control of iron influx and egress from cells. Although the mechanisms of its import into cells by iron carrier molecules are well characterized, iron export remains poorly understood. The current paradigm envisages unique functions associated with specialized macromolecules for its cellular import (transferrin receptors) or export (ferroportin, also known as SLC40A1). Previous studies have revealed that iron-depleted cells recruit glyceraldehyde-3-phosphate dehydrogenase (GAPDH), a multitasking, 'moonlighting' protein, to their surface for internalization of the iron carrier holotransferrin. Here, we report that under the converse condition of intracellular iron excess, cells switch the isoform of GAPDH on their surface to one that now recruits iron-free apotransferrin in close association with ferroportin to facilitate the efflux of iron. Increased expression of surface GAPDH correlated with increased apotransferrin binding and enhanced iron export from cells, a capability lost in GAPDH-knockdown cells. These findings were confirmed *in vivo* utilizing a rodent model of iron overload. Besides identifying for the first time an apotransferrin receptor, our work uncovers the two-way switching of multifunctional molecules to manage cellular micronutrient requirements.

KEY WORDS: Apotransferrin, Ferroportin, GAPDH, Iron export, Higher order multifunctional protein, Receptor

INTRODUCTION

Although iron (Fe^{2+}, Fe^{3+}) is an essential micronutrient for all life it can be a double-edged sword. It constitutes an essential component of various proteins that are crucial for oxygen transport and electron transfer. At the same time, excess iron catalyses the formation of highly reactive free radicals (through Fenton's reaction), which damage biomolecules through peroxidation (Dunn et al., 2007; Ganz, 2007; Hentze et al., 2004; Knutson and Wessling-Resnick, 2003). The accumulation of iron in cells and tissues causes medical complications, including cirrhosis, liver cancer, pancreatic failure, cardiomyopathy and arthritis (Burke et al., 2001; Kong et al., 2008). Iron overload also affects the central nervous system and has been implicated in the pathogenesis of Parkinson's and Alzheimer's diseases (Fleming and Ponka, 2012; Kong et al., 2008). It is therefore imperative for organisms to constantly maintain control of iron metabolism at all the different steps involving iron turnover. This involves tight regulation of the absorption (enterocytes), usage (erythroid cells), recycling (reticuloendothelial cells) and storage (macrophages and hepatocytes) of iron (Fleming and Ponka, 2012).

Practically all of extracellular iron in blood is chelated to transferrin, an abundant serum iron transport protein. Under physiological conditions, ~30% of the total transferrin is saturated with iron, leaving no excess free iron available to cause toxicity (Sheftel et al., 2012). Although the cellular iron uptake pathways through transferrin receptor proteins 1 and 2 [TfR1 (also known as CD71) and TfR2] are well characterized, knowledge regarding iron export is still limited (Ganz, 2007). Ferroportin [also known as iron-regulated transporter1 (IREG1), metal transporter protein 1 (MTP1) or SLC40A1] is the only known iron exporter in mammalian cells (Abboud and Haile, 2000; Donovan et al., 2000; McKie et al., 2000). It is expressed in duodenal enterocytes, tissue macrophages and hepatocytes, where it participates in cellular release of iron (Abboud and Haile, 2000; Canonne-Hergaux et al., 2006; Donovan et al., 2000; McKie et al., 2000; Ramey et al., 2010). Iron loading of cells enhances the localization of ferroportin to the plasma membrane of macrophages (Delaby et al., 2005); however, the exact mechanism by which ferroportin transports iron and how the exported iron is sequestered remains unclear (Ganz, 2007; Le Gac et al., 2013; Wessling-Resnick, 2006).

Previously it has been shown that the multifunctional glycolytic enzyme glyceradehyde-3-phosphate dehydrogenase functions as a receptor for holotransferrin (i.e. iron-saturated transferrin) and lactoferrin (also known as lactotransferrin) on the surface of a diverse range of cell types, including macrophages, and upon iron starvation many cells prefer to use surface-localized GAPDH for holotransferrin uptake rather than TfR1 (Kumar et al., 2012; Modun et al., 1998; Modun et al., 2000; Raje et al., 2007; Rawat et al., 2012). Recently, we have also demonstrated that cells enhance their secretion of GAPDH into the extracellular milieu (sGAPDH) when they are depleted of iron. This sGAPDH functions as an autocrine and/or paracrine receptor that traffics holotransferrin into various tissues and cell types (Sheokand et al., 2013). In the current study, we report an additional dimension to the multifunctionality of GAPDH, whereby the same protein demonstrates contrasting behavior under the opposing condition of cellular iron status (i.e. excess intracellular iron) to maintain iron homeostasis. Using cell types that play a key role in maintaining iron homeostasis (cells of the reticuloendothelial system, hepatocytes and enterocytes) we provide evidence that, when exposed to iron overload, cells again enhance their recruitment of GAPDH to the membrane

[1]Institute of Microbial Technology, CSIR, Sector 39A, Chandigarh, INDIA-160036. [2]National Institute of Pharmaceutical Education and Research, Phase X, Sector 67, SAS Nagar, Punjab, INDIA-160062.

*Author for correspondence (manoj@imtech.res.in)

Received 6 April 2014; Accepted 17 July 2014

Journal of Cell Science (2014) 127, 4279–4291 doi:10.1242/jcs.154005

surface. However, this GAPDH is an alternate isoform, which differs from that recruited upon iron starvation. It does not bind to holotransferrin; instead, it interacts with apotransferrin with high affinity and facilitates the export of iron from cells. This capability is lost in cells where GAPDH knockdown is performed. We further demonstrate that in iron loaded cells GAPDH interacts with ferroportin on the cell surface, which might facilitate the loading of iron exported by ferroportin onto apotransferrin. The results from our cell culture experiments were validated *in vivo* utilizing rodent models of iron overload.

RESULTS

Modulation of cell-surface GAPDH upon iron overload

Previously, we have demonstrated that iron starvation enhances surface GAPDH expression and many cells prefer this portal for holotransferrin acquisition instead of the well-studied TfR1 (Kumar et al., 2012). We were interested to investigate the response of this receptor system under conditions of iron excess in cells. To this end, we first confirmed cellular iron loading by two independent methods. Cells that play a key role in iron homeostasis were monitored for increased intracellular iron levels upon incubation with iron. A gradual increase in intracellular iron peaking at 12 hours was observed (supplementary material Fig. S1A). In addition, iron loading of macrophages was also achieved by erythrophagocytosis (EPG), a phenomenon that occurs naturally in organisms during clearance and recycling of effete erythrocytes (supplementary material Fig. S1B, and inset).

Surface TfR1 expression decreased in iron-loaded cells (supplementary material Fig. S1C,D), which is consistent with earlier reports of cells trying to limit further iron import (Auriac et al., 2010; Casey et al., 1988). At the same time, we detected an increased surface expression of GAPDH on primary macrophages, hepatocytes and macrophage cell lines, along with a decrease in the case of primary enterocytes (Table 1). *In vivo* experiments gave similar results. Peritoneal macrophages harvested from mice that had been injected intraperitoneally with iron dextran or opsonized red blood cells (RBCs) also demonstrated enhanced surface GAPDH (Table 1). The increase in surface GAPDH was time and dose dependent with respect to iron loading and did not involve any change in intracellular GAPDH levels (Fig. 1A,B). Previously, we have reported an increase in the amount of GAPDH on the surface of iron-starved cells (Kumar et al., 2012; Raje et al., 2007). When compared with those observations, we noticed that the extent of increase in GAPDH expression on the membrane was significantly higher upon iron loading of cells as compared with that observed during iron depletion (Fig. 1C).

GAPDH expressed on the cell membranes of iron-overloaded cells is of a different form than that observed upon iron starvation

To determine whether there was any difference in the nature of GAPDH expressed on cell surface upon iron overload as compared with that observed during iron depletion, we looked at the membrane partitioning of GAPDH in the two cases. Our previous work has demonstrated an increase in the FCDR ratio [the ratio of flow cytometric signal of the target molecule in the detergent-resistant membrane fraction (DRM) versus total signal (Gombos et al., 2004)] of GAPDH upon iron starvation of cells, indicating that the GAPDH present on the cell surface upon cellular iron depletion is preferentially localized to the detergent-resistant fraction of the membrane (Kumar et al., 2012). Interestingly, in the case of iron-overloaded cells, although the amount of surface GAPDH increased to a greater extent, no significant change in the FCDR ratio, as compared with that of control cells, could be observed (Fig. 1D,E), suggesting that the increased GAPDH is equally distributed between both membrane fractions. Analysis of membrane protein fractions by two-dimensional (2D) gel electrophoresis and western blotting revealed an alkaline shift in the predominant GAPDH isoforms of iron-loaded cells as compared with those of iron-depleted cells (Fig. 1F). Liquid chromatography-tandem mass spectrometry (LC-MS/MS) analysis of membrane-associated GAPDH from iron-depleted cells revealed a higher abundance of numerous post-translational modifications (PTMs), including oxidation, dimethylation, acetylation, nitrosylation and phosphorylation, as compared with GAPDH from the membranes of iron-loaded cells (Fig. 2A–C).

The increase in surface GAPDH upon iron overload also did not result in any increase in the cellular capacity to bind to

Table 1. Fold change in surface expression of GAPDH and apotransferrin binding upon iron overload as compared with control cells at 24 hours

Experimental iron overload		Cell type	Surface GAPDH	Apotransferrin binding
Ex vivo	$FeCl_3$	Rat hepatocytes	2.70	1.84
		Rat peritoneal macrophages	4.00	2.17
		Rat spleen macrophages	1.83	1.45
		Rat enterocytes	0.75	0.74
		J774	3.38	2.77
		RAW	1.78	1.59
		THP1	2.41	1.94
		GAPDH-knockdown THP1	ND#	ND#
	Erythrocyte phagocytosis	Rat spleen macrophages	1.46	1.56
		J774	2.40	2.00
		THP1	1.77	1.52
		GAPDH-knockdown THP1	ND#	ND#
In vivo	Iron dextran	Rat peritoneal macrophages	1.48	1.62
	Erythrocyte phagocytosis	Rat peritoneal macrophages	2.06	5.50

Different cell types were subjected to iron overload either *ex vivo* (by $FeCl_3$ or RBC phagocytosis for 24 hours) or by intraperitoneal injection of iron dextran or opsonized erythrocytes into male Sprague-Dawley rats. Peritoneal macrophages were isolated at 24 hours. Controls were set up in parallel (see Materials and Methods for details). The surface expression of GAPDH and apotransferrin binding was evaluated by flow cytometry; $P<0.0001$ in all cases except those marked with a hash (#). ND, not detectable; $n=10^4$ cells in each case; all experiments repeated at least three times.

Journal of Cell Science (2014) 127, 4279–4291 doi:10.1242/jcs.154005

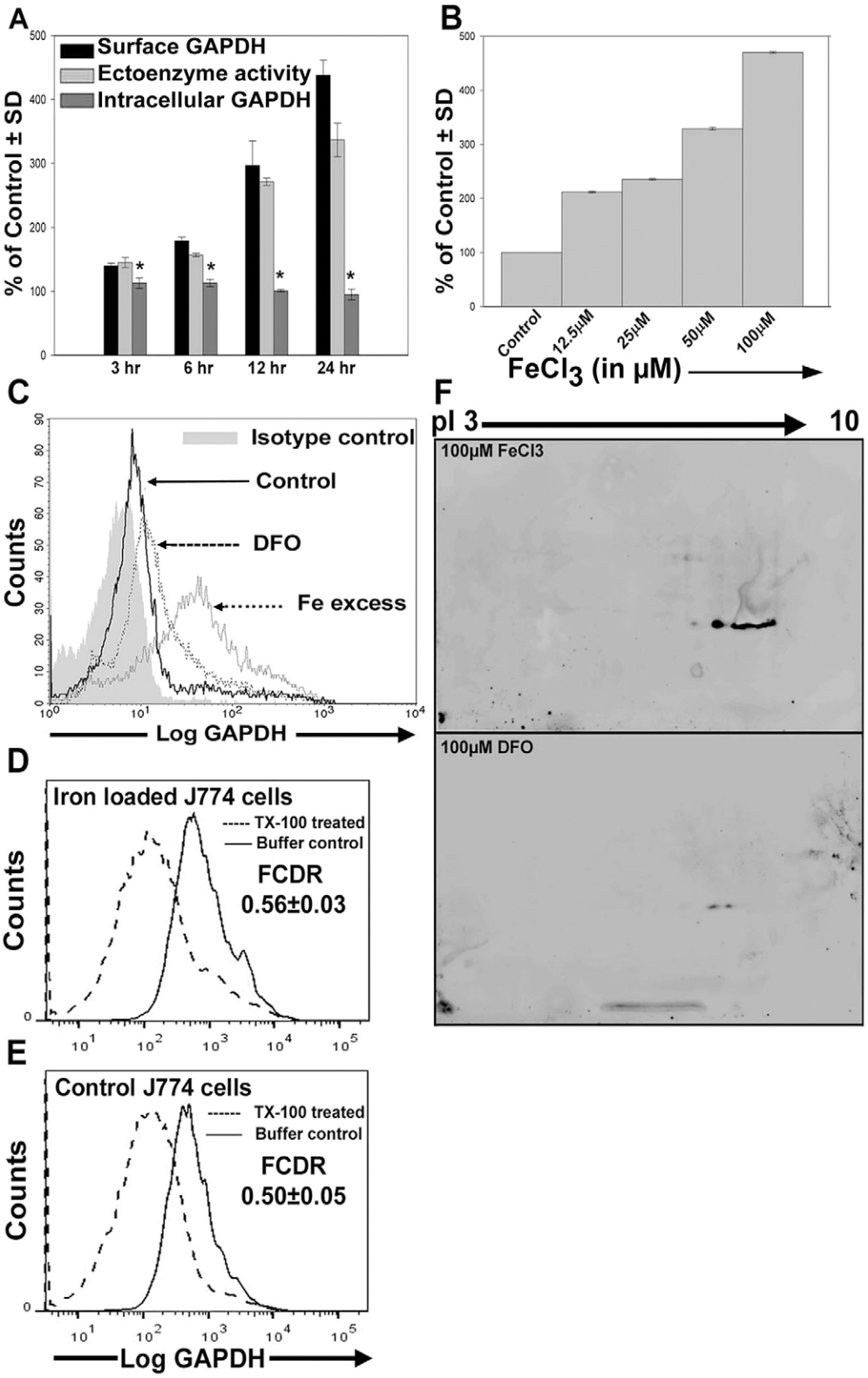

Fig. 1. Modulation and characterization of surface GAPDH upon iron loading of cells. (A) J774 cells were cultured in 100 μM-$FeCl_3$-supplemented medium for increasing time periods and checked for changes in surface-associated GAPDH as well as intracellular expression of GAPDH by flow cytometric analysis. Extracellular GAPDH was also monitored for ectoenzyme activity. Surface and intracellular GAPDH data are presented as a percentage of the mean fluorescence intensity of control samples; $P<0.005$; $^*P>0.05$; $n=10^4$ cells. For ectoenzyme activity, data are presented as a percentage of the OD at 340 nm of the control sample; $P<0.0005$; $n=4$ independent experiments. (B) J774 cells were treated with increasing concentrations of iron up to 100 μM $FeCl_3$, and the surface expression of GAPDH was evaluated. Data are presented as a percentage of the mean fluorescence intensity of control samples; $P<0.0001$; $n=10^4$ cells. (C) The increase in the amount of cell surface GAPDH is significantly larger upon iron loading of cells compared with that observed following iron depletion. J774 cells were treated with either 100 μM $FeCl_3$ or 100 μM DFO for 24 hours before flow-cytometry-based analysis of surface GAPDH; $P<0.0001$; $n=10^4$ cells. (D,E) GAPDH is present in both DRM and non-DRM membrane fractions in control as well as iron-loaded J774 cells; $P<0.0001$ (statistical analysis was performed using mean fluorescence intensities); $n=10^4$ cells. (F) Western blot of 2D-gel-electrophoresis-separated GAPDH isoforms from membrane fractions of iron-loaded (100 μM $FeCl_3$) and iron-depleted (100 μM DFO) J774 cells. pI, isoelectric point. Also see supplementary material Fig. S1.

holotransferrin as reported previously for iron-depleted cells (Kumar et al., 2012); in fact, there is a significant decrease (Fig. 3A). These results collectively demonstrate that GAPDH recruited to the cell surface during iron overload is a different isoform than that presented upon iron starvation.

Modulation of apotransferrin binding upon iron overload

As excess iron is deleterious, iron-loaded cells would seek to divest themselves of this excess of metal. Apotransferrin, abundantly present in serum, is among the best known biological chelators of iron, and we checked for its recruitment

Journal of Cell Science (2014) 127, 4279–4291 doi:10.1242/jcs.154005

A Membrane GAPDH from iron depleted cells

1 MVKVGVN$_{(deamid)}$GFGRIGRLVTRAAICSGKVEIVAIN$_{(deamid)}$DPFID$_{(methyl)}$LN$_{(deamid)}$YM$_{(ox)}$VYMFQYDST
51 HGKFNGTVKAENGKLVIN$_{(deamid)}$GKPITIFQ$_{(deamid)}$ERDPTNIKWGEAGAEYVVESTGVF
101 TTM$_{(ox)}$EKAGAHLKGGAKRVIISAPSADAP$_{(pro\text{-}pyro\text{-}glu)}M_{(ox)}FVM_{(ox)}GVN_{(deamid)}HEK_{(acetyl)}YDN_{(deamid)}SLK_{(acetyl)}$IVSNASC
151 TTN$_{(deamid/dimethyl)}$C$_{(ox/nitrosyl)}$LAPLAKVIHDN$_{(deamid/dimethyl)}$FGIVEGLM$_{(ox)}$TTVHAITATQKTVDGPSGKLWRDGRGA
201 AQNIIPASTGAAKAVGKVIPELN$_{(deamid)}$GKLTGMAFRVP$_{(pro\text{-}pyro\text{-}glu)}TP_{(pro\text{-}pyro\text{-}glu)}$NVSVVDLT$_{(phos)}C_{(nitosyl/propionamide)}$RLEKP
251 AKYDDIKKVVKQ$_{(deamid)}$ASEGPLKGILGYTEDQVVSC$_{(propionamide)}$DFN$_{(dimethyl)}$SN$_{(dimethyl)}$SHSSTFDAGAGIA
301 LN$_{(deamid)}$DNFVKLISWYDNEYGYSN$_{(deamid)}$RVVDLMAYM$_{(ox)}$ASKE$_{(methyl)}$

B Membrane GAPDH from iron treated cells

1 MVKVGVN$_{(deamid)}$GFGRIGRLVTRAAICSGKVEIVAIN$_{(deamid)}$DP$_{(pro\text{-}pyro\text{-}glu)}$FIDLN$_{(deamid)}$YMVYMFQ$_{(deamid)}$YDST
51 HGKFNGTVKAENGKLVIN$_{(deamid)}$GKPITIFQ$_{(deamid)}$ERDPTNIKWGEAGAEYVVESTGVF
101 TTMEKAGAHLKGGAKRVIISAPSADAPM$_{(ox)}$FVMGVN$_{(deamid)}$HEKYDN$_{(deamid)}$SLKIVSNASC
151 TTN$_{(deamid/dimethyl)}$C$_{(nitrosyl)}$LAPLAKVIHDNFGIVEGLM$_{(ox)}$TTVHAITATQ$_{(deamid)}$KTVDGPSGKLWRDGRGA
201 AQNIIPASTGAAKAVGKVIPELN$_{(deamid)}$GKLTGMAFRVPTPN$_{(deamid)}$VSVVDLTC$_{(propionamide)}$RLEKP
251 AKYDDIKKVVKQASEGPLKGILGYTEDQVVSC$_{(propionamide)}$D$_{(methyl)}$FNSNSHSSTFD$_{(methyl)}$AGAGIA
301 LNDNFVK$_{(dimethyl)}$LISWYDNEYGYSNRVVDLMAYM$_{(ox)}$ASKE$_{(methyl)}$

C

PTMs	GAPDH (iron depleted)	GAPDH (iron treated)
Methylation(D,E)	2 [D_{37}, E_{333}]	3 [D_{283}, D_{294}, E_{333}]
Dimethylation(N,R,K)	4 [N_{153}, N_{165}, N_{285}, N_{287}]	2 [N_{153}, K_{307}]
Deamidation(N,Q)	13 [N_7, N_{32}, N_{39}, N_{68}, Q_{76}, N_{134}, N_{140}, N_{153}, N_{165}, N_{223}, Q_{262}, N_{302}, N_{320}]	12 [N_7, N_{32}, N_{39}, Q_{46}, N_{68}, Q_{76}, N_{134}, N_{140}, N_{153}, Q_{183}, N_{223}, N_{237}]
Oxidation(M,C)	7[M_{41}, M_{103}, M_{128}, M_{131}, C_{154}, M_{173}, M_{329}]	3[M_{128}, M_{173}, M_{329}]
Phosphorylation(S,T,Y)	1[T_{244}]	ND*
Acetylation(K)	2[K_{137}, K_{143}]	ND*
Nitrosylation(C)	2[C_{154}, C_{245}]	1[C_{154}]
Propionamide(C)	2[C_{245}, C_{282}]	2[C_{245}, C_{282}]
Pro- pyro glu(P)	3[P_{127}, P_{234}, P_{236}]	1[P_{34}]
Succinylation(K),	ND*	ND*
ADP-ribosylation(C),	ND*	ND*
Palmitoylation(C),	ND*	ND*
GPI anchor(protein C term),	ND*	ND*
Farnesylation(C),	ND*	ND*
Myristoylation(Nterm G),	ND*	ND*
Pyro-Glu(E, Q)	ND*	ND*

* Not Detected

Fig. 2. LC-MS/MS analysis of membrane-associated GAPDH from iron-depleted and iron-loaded cells. J774 cells were cultured in medium supplemented with 100 μM $FeCl_3$ or 100 μM DFO for 24 hours, and membrane fractions were purified. Membrane proteins from both samples were extracted and subjected to 12% SDS-PAGE. Bands corresponding to GAPDH were excised and trypsin digested. Peptide analysis by Mascot following LC-MS/MS confirmed proteins to be GAPDH. The MOWSE score was >700, with sequence coverage of >80% in both cases. (A) PTMs observed in GAPDH recruited to the cell membrane upon iron depletion in J774 cells. (B) PTMs observed in GAPDH recruited to the cell membrane upon iron overload in J774 cells. (C) Comparative analysis of various PTMs and the corresponding modified residues in GAPDH recruited to the cell membrane under both conditions.

to iron-loaded cells. Macrophages and hepatocytes demonstrated an increased binding of apotransferrin, which correlated with the increase in surface GAPDH expression (Fig. 1A–D; Fig. 3B; Table 1). In the case of primary enterocytes, surface GAPDH decreased along with a corresponding decrease in apotransferrin binding (Table 1). GAPDH-knockdown THP1 cells, which fail to enhance surface GAPDH upon iron overload, also lacked apotransferrin binding (Table 1). The increase in apotransferrin binding by cells also matched the time-dependent increase in the amount of surface GAPDH upon iron loading (Fig. 3C; Fig. 1A).

Apotransferrin binding to cells

The equilibrium dissociation constant (K_D) of apotransferrin binding to the surface of excess-iron-treated J774 cells was calculated to be 1.11 nM (Fig. 3D), suggesting the presence of a high-affinity receptor. This is similar to the value of 1 nM reported for TfR1, and there could be some concern that the affinity reported in this case is due to transferrin binding to TfR1 either in the apo form or after conversion into holotransferrin. However, TfR1 does not bind to apotransferrin at physiological pH (Andrews, 2000), and apotransferrin was prevented from conversion to the holo form by the inclusion of desferrioxamine (DFO) in the incubation buffer (Kawabata et al., 2000). Flow cytometric analysis demonstrated that apotransferrin binding to cells is inhibited in the presence of excess of unlabeled ligand (Fig. 3E), indicating that it is a specific process. In addition, the binding was decreased when cells were pretreated with the proteolytic enzyme pronase (Fig. 3F), confirming that the receptor involves a protein molecule (Kumar et al., 2012).

GAPDH and apotransferrin interact *in vitro*

As surface GAPDH appeared to be a receptor for apotransferrin binding on iron-loaded cells, we decided to first check whether GAPDH and apotransferrin interact *in vitro*. To evaluate this, plate-based solid-phase interaction and surface plasmon resonance (SPR) assays were performed. GAPDH coated in enzyme-linked immunosorbent assay (ELISA) wells specifically captured apotransferrin (supplementary material Fig. S2A). A Biacore assay revealed a K_D of 5.3 nM for the GAPDH–apotransferrin interaction (supplementary material Fig. S2B).

GAPDH and apotransferrin colocalize and interact on the cell surface

To ascertain whether this strong *in vitro* interaction of GAPDH and apotransferrin occurs *in vivo*, we investigated the association and interaction of GAPDH with apotransferrin on the surface of iron-treated J774 cells. Utilizing confocal microscopy, GAPDH was observed to colocalize with apotransferrin on the surface of

Journal of Cell Science (2014) 127, 4279–4291 doi:10.1242/jcs.154005

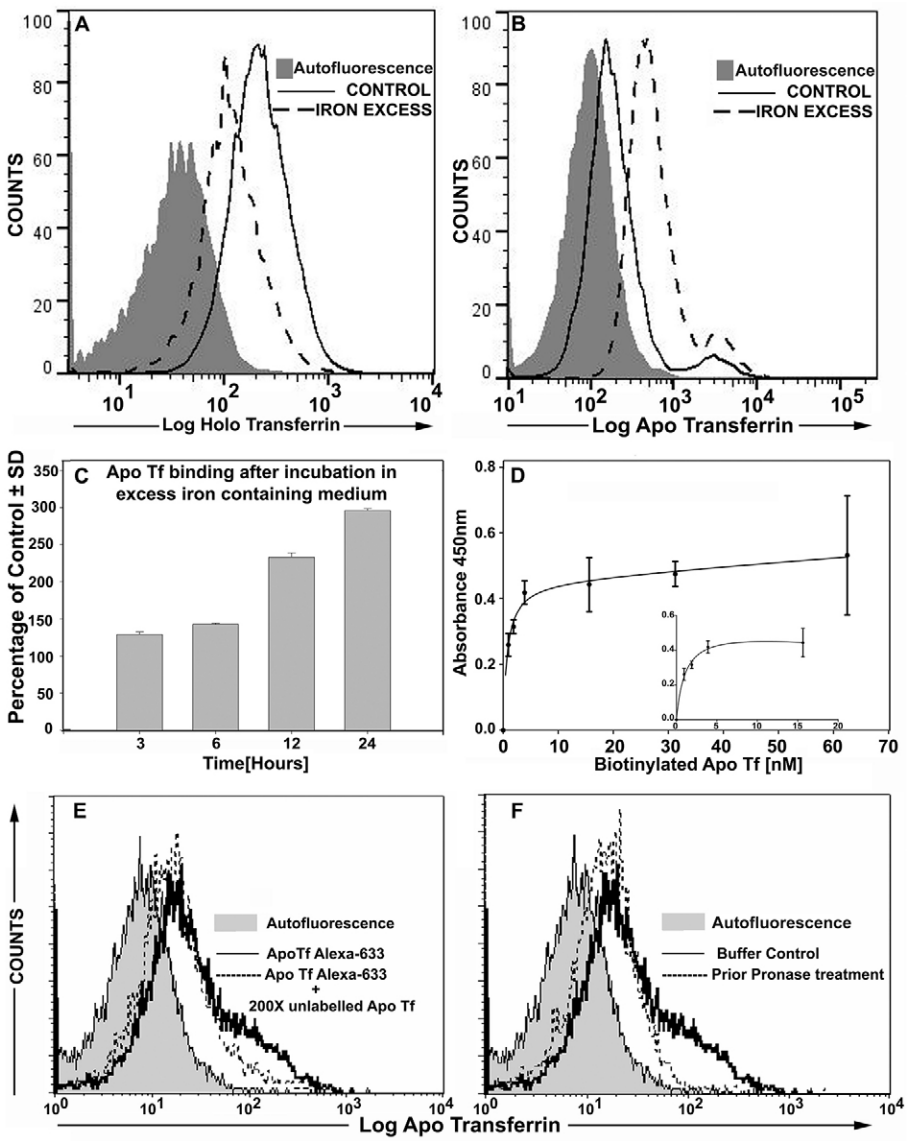

Fig. 3. The binding of apotransferrin to iron-loaded cells is selectively enhanced. (A) There is a significant decrease in cell-surface holotransferrin–Alexa-Fluor-647 binding by iron-loaded J774 cells; $P<0.05$; $n=10^4$ cells. (B) Apotransferrin–Alexa-Fluor-647 binding is increased on the surface of iron-loaded J774 cells; $P<0.0001$; $n=10^4$ cells. (C) The magnitude of the increase in apotransferrin (Apo Tf) binding increases with the length of exposure to iron. J774 cells were treated with 100 μM $FeCl_3$ for increasing lengths of time and the binding of apotransferrin–Alexa-Fluor-647 was measured. The data are presented as a percentage of mean fluorescence intensity of control samples; $P<0.005$; $n=10^4$ cells. (D) Concentration-dependent binding of apotransferrin on the surface of iron-loaded J774 cells. The results are expressed as the concentration of biotinylated apotransferrin versus OD at 450 nm (±s.d.). (E,F) The binding of apotransferrin to the surface of iron-treated J774 cells is specific (E) and pronase sensitive (F); $P<0.0001$; $n=10^4$ cells. All experiments were repeated three times.

cells (Fig. 4A; supplementary material Fig. S2C,D). An acceptor-photobleaching-based Foster resonance energy transfer (FRET) assay also demonstrated an interaction between surface GAPDH and apotransferrin (Fig. 4B,C; supplementary material Fig. S2E). Finally, co-immunoprecipitation of biotinylated apotransferrin with GAPDH from the membranes of iron-loaded cells confirmed the interaction between the two proteins (Fig. 4D).

Correlated modulation of surface GAPDH and apotransferrin binding in iron-loaded rats

We utilized an *in vivo* rat model to determine whether iron loading indeed increases cell-surface GAPDH and apotransferrin binding. Liver and serum iron estimation confirmed the iron overload in a rat model (supplementary material Fig. S3A,B). Hepatocytes, peritoneal macrophages and enterocytes were examined for surface expression of GAPDH and apotransferrin binding as compared with that of cells isolated from control animals. Whereas hepatocytes and peritoneal macrophages of iron-loaded rats demonstrated an increase in surface GAPDH expression along with a corresponding increase in apotransferrin binding, enterocytes demonstrated a decrease in both surface expression of GAPDH and apotransferrin binding (Fig. 5A; supplementary material Fig. S3C). The change in cell-surface expression of GAPDH upon iron loading correlated well with the change in apotransferrin binding by all three cell types studied (Fig. 5B).

Apotransferrin recruited by GAPDH facilitates iron export

To understand the physiological significance of increased apotransferrin capture by iron-loaded cells, we explored its role in the facilitation of iron export from cells. Having established that incubation with iron-supplemented medium causes maximum intracellular iron accumulation within 12 hours (supplementary material Fig. S1A), we chose this as a starting point from which to evaluate iron exit. When apotransferrin was included in the incubation medium, iron-loaded J774 cells demonstrated a significant enhancement of iron export into the extracellular medium within 1 hour, as assayed by the chromogenic iron assay (supplementary material Fig. S4A). Exit of iron was also quantified using cells labeled with ^{55}Fe. We observed an increase in iron export from various iron-loaded (by $FeCl_3$ incubation or EPG) cells when incubated with apotransferrin (Fig. 6A,B). J774 and THP1 cells that had not been subjected to any iron loading (untreated control cells) also demonstrated a

Journal of Cell Science (2014) 127, 4279–4291 doi:10.1242/jcs.154005

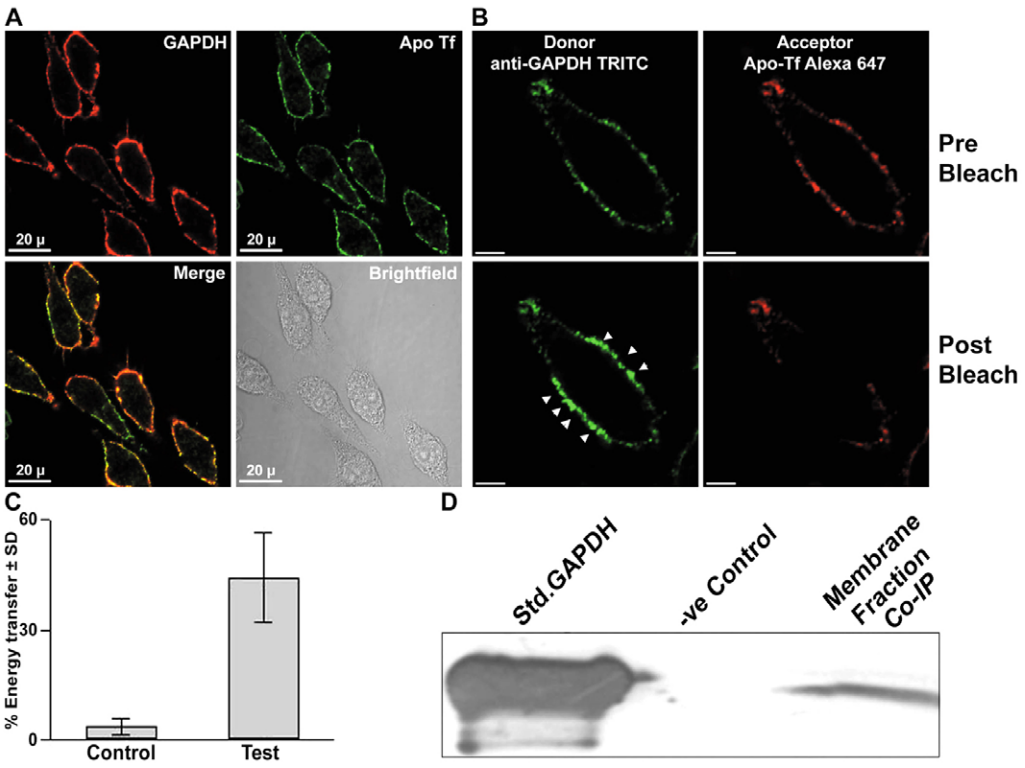

Fig. 4. Cell-surface GAPDH interacts with apotransferrin on the cell surface. (A) Colocalization of GAPDH and apotransferrin–FITC (Apo Tf) on the surface of excess-iron-treated J774 cells, as determined using confocal microscopy. Pearson's correlation coefficient is 0.94; also see supplementary material Fig. S2C,D. GAPDH was detected with the mouse monoclonal anti-GAPDH antibody and anti-mouse-IgG–Alexa-Fluor-568. Scale bars: 20µm. (B) GAPDH on the surface of excess-iron-treated J774 cells interacts with apotransferrin as seen by FRET signal, which is represented by an increase (arrowheads) in donor signal (anti-GAPDH–TRITC) upon bleaching of the acceptor (apotransferrin–Alexa-Fluor-647). Scale bars: 5 µm. (C) FRET efficiency [signal intensity of ($Donor_{post\ Bleach}$−$Donor_{pre\ Bleach}$)/$Donor_{post\ Bleach}$×100] was compared to that of control, where instead of apotransferrin–Alexa-Fluor-647 the unrelated goat-IgG–Alexa-Fluor-647 was used; $P<0.0001$; $n=25$ cells. (D) Excess-iron-treated J774 cells were incubated with biotinylated apotransferrin at 4˚C, and the membrane fraction was prepared and subjected to co-immunoprecipitation (Co-IP) using streptavidin–Magnabeads. The interaction between GAPDH and apotransferrin was confirmed by western blotting using monoclonal anti-GAPDH antibody. A negative (-ve) control was run in parallel, wherein the incubation of cells with biotinylated apotransferrin was omitted. Std., standard (rabbit muscle GAPDH). See also supplementary material Fig. S2.

small baseline change in iron export when apotransferrin was added into the incubation medium (supplementary material Fig. S4B). Interestingly, incubation with apotransferrin caused a sharp increase in iron export from untreated enterocytes, whereas in iron-loaded enterocytes the effect of apotransferrin was minimal (supplementary material Fig. S4B; Fig. 6A). The addition of apotransferrin failed to enhance iron export from untreated or iron-loaded GAPDH-knockdown THP1 cells (Fig. 6A,B; supplementary material Fig. S4B). In addition, this effect of apotransferrin in enhancing iron exit was dose dependent and could not be brought about by holotransferrin (Fig. 6C). We further confirmed that the iron exported out of cells is sequestered into apotransferrin (Fig. 6D) by precipitating the added apotransferrin and checking for the presence of protein-bound radioactive iron.

Surface GAPDH colocalizes and interacts with ferroportin

Ferroportin, the only known iron exporter in mammals, is known to localize to the cell membrane upon iron loading (Delaby et al., 2005). Having observed that, in iron-loaded cells, surface GAPDH recruits apotransferrin to facilitate cellular iron export (Figs 4–6), we decided to evaluate the possibility of any GAPDH–ferroportin interaction on the surface of these cells. Confocal microscopy demonstrated the simultaneous colocalization of all three proteins on cells (Fig. 7A). Acceptor-photobleaching-based FRET analysis demonstrated the interaction between GAPDH and ferroportin (Fig. 7B–D). Finally, co-immunoprecipitation of surface GAPDH and ferroportin confirmed the interaction between the two proteins (Fig. 7E).

DISCUSSION

Iron metabolism has long been an area of active research (Ganz, 2013) and, although extensive studies have been conducted to characterize the mechanistic basis of iron import by cells, the field of cellular iron export is still poorly explored. In our earlier studies, when cells were depleted of iron, we observed an increase in the recruitment of GAPDH to the cell surface, which enhanced holotransferrin trafficking, demonstrating the role of GAPDH in maintaining essential levels of cellular iron (Kumar et al., 2012; Raje et al., 2007). To fully comprehend its role in iron homeostasis, we investigated how this molecule responds when cells are loaded with iron (under such situations TfR1 expression on cells is known to be downregulated). Interestingly, we once again observed an increase (to an even greater extent than was observed upon iron depletion) in the surface expression of GAPDH in macrophages and hepatocytes. Unlike our earlier observations in iron-starved cells (Kumar et al., 2012), and also in agreement with an earlier report showing that iron loading did not

Journal of Cell Science (2014) 127, 4279–4291 doi:10.1242/jcs.154005

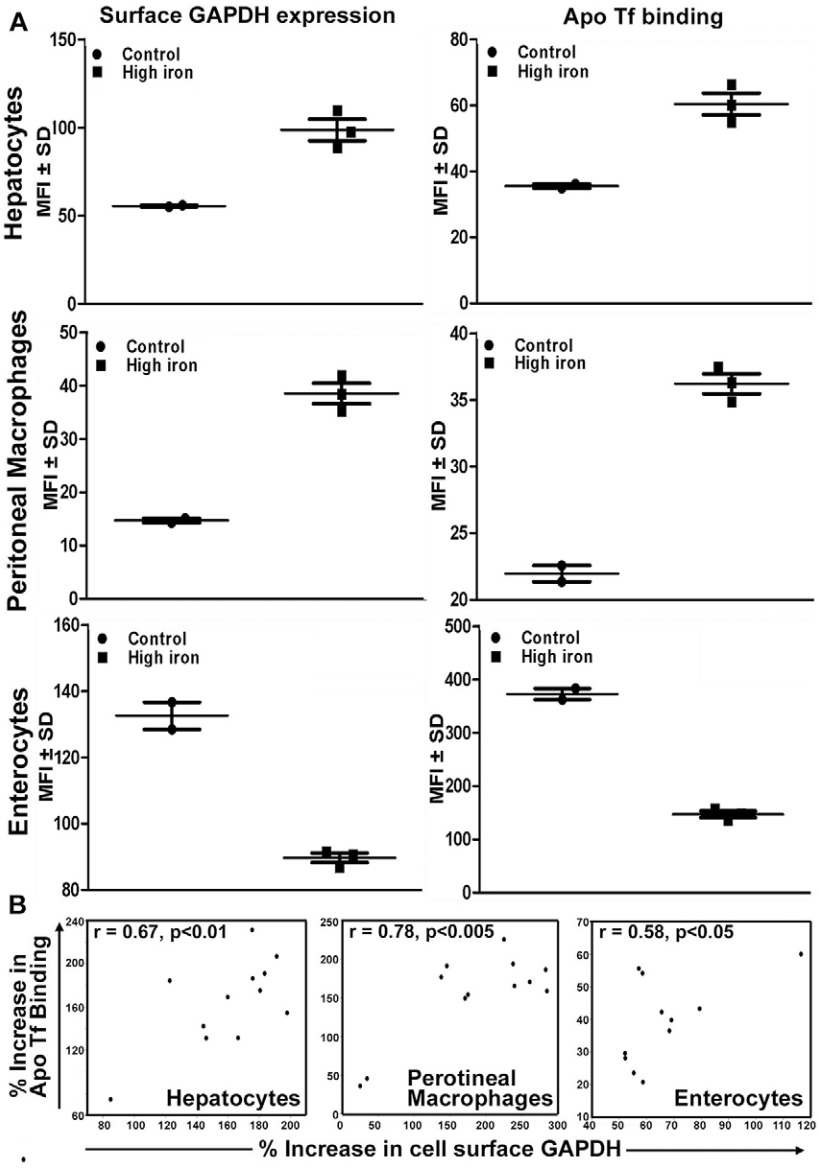

Fig. 5. Modulation of cell-surface GAPDH and apotransferrin binding in cells isolated from chronically iron-loaded Sprague-Dawley rats. (A) Primary hepatocytes and peritoneal macrophages isolated from iron-loaded rats demonstrate increases in both surface GAPDH expression and apotransferrin (Apo Tf) binding as compared with that of cells isolated from control rats; $P<0.05$ (hepatocytes), $P<0.002$ (peritoneal macrophages); $n=3$ test animals. Enterocytes isolated from iron-loaded rats showed a decrease in both surface GAPDH expression and apotransferrin binding in comparison to cells isolated from control rats; $P<0.001$; $n=3$. From each test animal, 10^4 cells were analyzed by flow cytometry for each parameter separately, and the results are presented as the mean fluorescence intensity (MFI)± s.d. The data are representative of five independent experiments (see supplementary material Fig. S3 for results of all five groups). (B) Correlation between the change in expression of surface GAPDH and apotransferrin binding to cells from all iron-loaded animals. See also supplementary material Fig. S3.

alter GAPDH expression in rat liver (Quail and Yeoh, 1995), no change in intracellular GAPDH levels upon iron loading was observed. These observations suggest that the increase in the amount of membrane-associated GAPDH could be due to redeployment of the existing intracellular protein to the membrane. Because membrane-associated GAPDH accounts for a tiny fraction of the vast pool of intracellular GAPDH (Seidler, 2013), no discernible alteration in cytosolic levels would be perceptible. Our results also demonstrate that the GAPDH recruited to the cell membrane upon iron overload is of a different isoform than that deployed upon iron depletion. The existence of discrete GAPDH isoforms catalyzing independent functional activities is well known (Glaser and Gross, 1995; Seidler, 2013), and a switching of GAPDH in the membrane of bone-marrow-derived macrophages upon iron loading to a more alkaline isoform has been reported recently (Polati et al., 2012). Our LC-MS/MS results demonstrate that GAPDH recruited upon iron loading lacks phosphorylation and acetylation and also has a lower abundance of several PTMs, including oxidation, dimethylation and nitrosylation in comparison to GAPDH recruited upon iron depletion. These modifications are well known for their ability to shift the isoelectric point of proteins as observed by us in this study, as well as by numerous other workers previously (Choudhary et al., 2000; Grillon et al., 2012; Kuyumcu-Martinez et al., 2007; Madian et al., 2012; Park et al., 1988; Zhang et al., 2011). The presence of numerous PTMs in GAPDH has been well established in earlier reports (Seidler, 2013; Seo et al., 2008).

Unlike the GAPDH recruited upon iron depletion (Kumar et al., 2012), GAPDH expressed on the membrane during iron overload does not bind to holotransferrin. This is expected as under these conditions cells are already coping with an excess of the metal and would seek to restrict further iron import through holotransferrin. By contrast, these cells have an urgent need to externalize their excess iron. As a high level of extracellular free iron is deleterious, the exported iron needs to be expeditiously chelated from the vicinity of the cell (Hentze et al., 2004). One of the most abundant and high-affinity chelators of iron in serum capable of this task is apotransferrin (Sheftel et al., 2012), and the existence of an independent apotransferrin receptor for such a

Journal of Cell Science (2014) 127, 4279–4291 doi:10.1242/jcs.154005

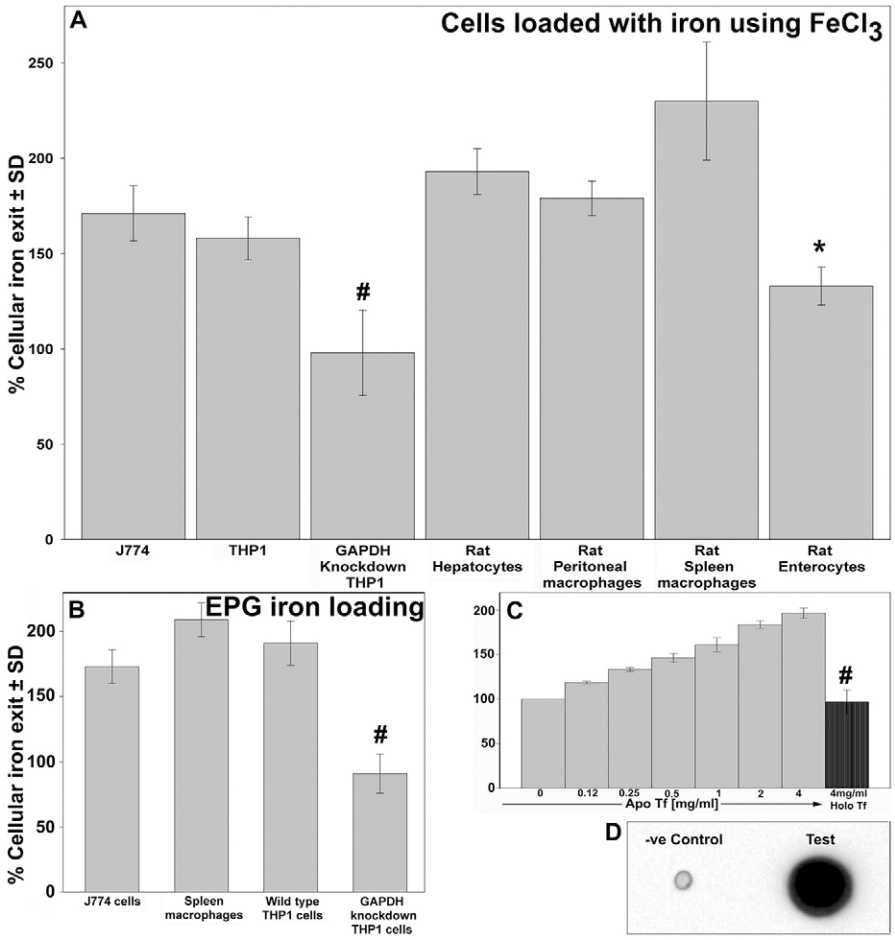

Fig. 6. GAPDH facilitates iron export by apotransferrin in iron-loaded cells. (A,B) Cell lines and rat primary cells were iron loaded using either treatment with 100 μM $FeCl_3$ (A) or EPG (B) in medium spiked with ^{55}Fe for 12 hours. Subsequent incubation of cells with apotransferrin (Apo Tf) resulted in enhanced iron export into the incubation medium as compared with that observed in cells where apotransferrin was omitted; $P<0.0005$, $^{*}P<0.001$, $^{\#}P>0.05$; $n=4$ experimental replicates. Data are presented as a percentage of counts per minute (CPM) in incubation medium of cells incubated without apotransferrin, shown as the mean±s.d.; each experiment was repeated multiple times. (C) The effect of apotransferrin in enhancing iron exit is dose dependent. J774 cells treated with 100 μM $FeCl_3$ (spiked with $^{55}FeCl_3$) were incubated with increasing concentrations of apotransferrin or 4 mg/ml holotransferrin (Holo Tf) (the maximum concentration of apotransferrin tested) and iron exit into the incubation medium was quantified; $P<0.0001$, $^{\#}P>0.05$; $n=4$ experimental replicates. Data are presented as a percentage of CPM in the incubation medium of cells incubated without apotransferrin, shown as the mean±s.d. (D) Iron released by cells is loaded onto apotransferrin. J774 cells loaded with iron as above were incubated with 0.5 mg/ml of biotinylated apotransferrin, and after immunoprecipitation of apotransferrin from cell supernatants with streptavidin–Magnabeads the captured radioactive iron was visualized on nitrocellulose membrane by phosphoimaging. A negative (-ve) control where incubation with biotinylated apotransferrin was omitted was run in parallel. See also supplementary material Fig. S4.

purpose has been suggested previously (Umbreit, 2005). We examined apotransferrin binding to the surface of iron-loaded cells and observed an increase upon iron loading. This correlated with the increased amount of surface GAPDH in various cells analyzed. Cells in which GAPDH had been knocked down, which thus did not express GAPDH on their surface, completely failed to bind to apotransferrin either under normal conditions or upon iron overload (Table 1). The binding of apotransferrin was modulated in a time-dependent manner similar to the increase in the amount of surface GAPDH. In addition, it was specific, saturable and pronase sensitive, demonstrating the involvement of a protein receptor with an affinity of ~1 nM. Earlier investigations have suggested the existence of such specific, saturable and pronase-sensitive binding of apotransferrin to rat peritoneal macrophages, involving very-high-affinity receptors and occurring independently of holotransferrin binding (Nishisato and Aisen, 1982). However, to date, no specific molecule has been identified as an apotransferrin receptor. Our data suggests that this high-affinity receptor for apotransferrin on the surface of macrophages is an isoform of GAPDH.

Biacore-based analysis revealed the affinity of the GAPDH–apotransferrin interaction to be of the same order as that of the transferrin–TfR1 interaction and also to correlate with the binding affinity of apotransferrin for iron-loaded cells. Confocal microscopy based colocalization, co-immunoprecipitation and FRET-based assays further confirmed the interaction of GAPDH and apotransferrin on cells. A study utilizing K562 cells suggested the existence of common apo and holotransferrin-binding sites (Xiu-Lian et al., 2004). However, K562 cells do not express GAPDH on their surface at all (Kumar et al., 2012), and those results might be due to the existence of some alternative binding sites.

Our studies provide evidence that the interaction of apotransferrin with iron-loaded cells facilitates the exit of iron and that this ability is lost upon knockdown of GAPDH. These results demonstrate that surface GAPDH and apotransferrin are crucial for iron egress. The role of apotransferrin in iron export has been demonstrated previously with mixed results. It enhanced iron release from rat Kupffer cells, bone marrow macrophages (Kondo et al., 1988; Rama et al., 1988) and hypoxic macrophages in the presence of ceruloplasmin (Sarkar et al., 2003). *In vivo* studies have demonstrated that iron infused to decrease plasma iron-binding capacity (by decreasing levels of serum apotransferrin) reduces post-EPG cellular iron release (Bergamaschi et al., 1986; Lipschitz et al., 1971; Siegenberg et al., 1990), and rat bone marrow macrophages exhibit a suppressed iron release when incubated with saturated transferrin (Rama et al., 1988). However, other groups have reported that apotransferrin has no effect on iron release after infusion of RBCs (Lipschitz et al., 1971) or after EPG in isolated rat peritoneal macrophages (Saito et al., 1986).

As ferroportin is a well-established iron exporter in mammals, we investigated whether surface GAPDH interacts with ferroportin and confirmed this to be the case in iron-loaded macrophages. We hypothesize that GAPDH recruits

Journal of Cell Science (2014) 127, 4279–4291 doi:10.1242/jcs.154005

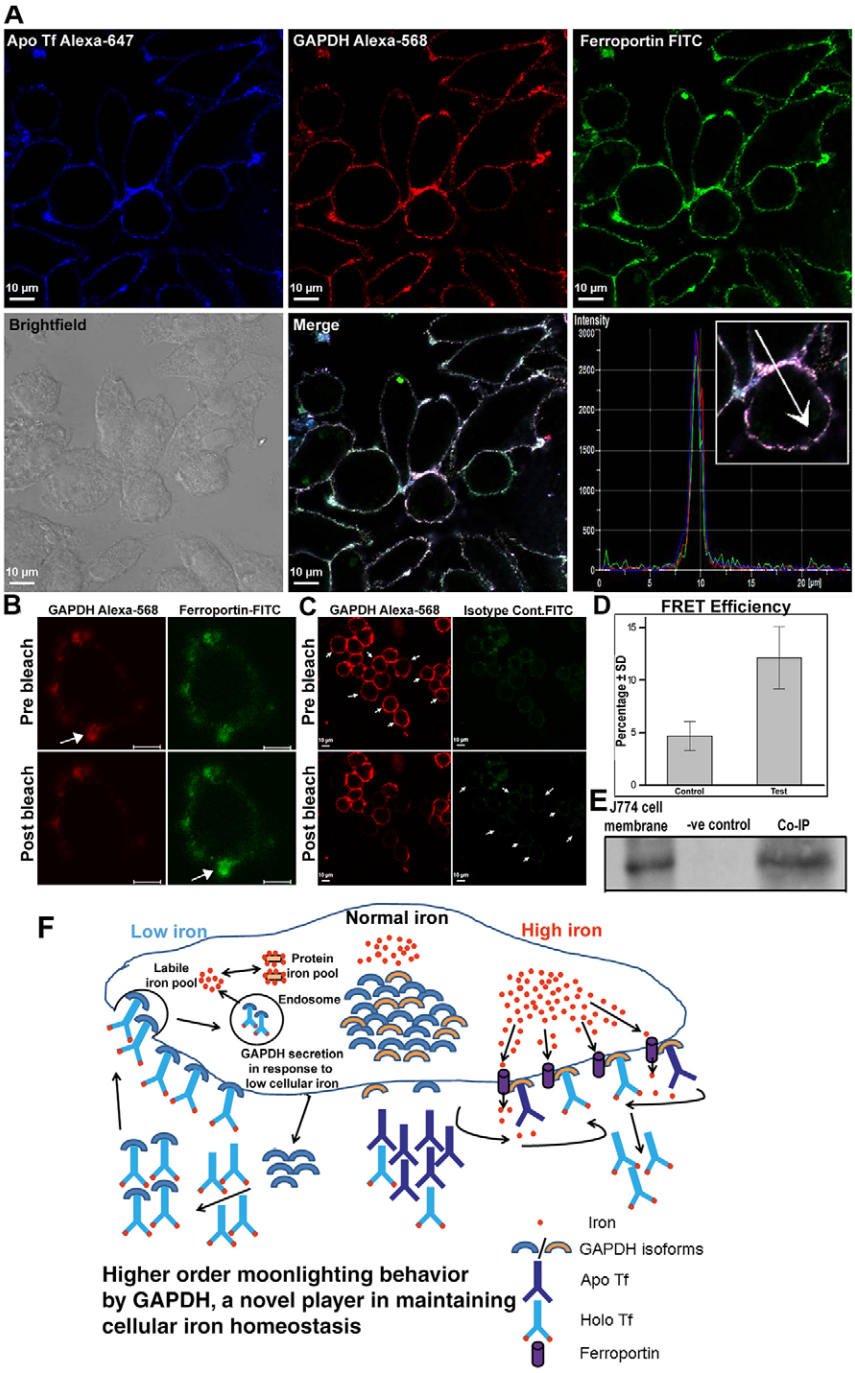

Fig. 7. GAPDH and ferroportin interact at the surface of iron-loaded J774 cells. (A) Colocalization of GAPDH, ferroportin and apotransferrin (Apo Tf) on the surface of iron-treated J774 cells by confocal microscopy. Pearson's correlation coefficient is 0.92 for the localization of ferroportin with GAPDH and apotransferrin, and 0.95 for that of GAPDH with apotransferrin. (B) GAPDH on the surface of iron-loaded J774 cells interacts with ferroportin as observed by FRET signal (arrows), represented by an increase in donor signal (ferroportin) upon bleaching of the acceptor (GAPDH). Scale bars: 5 μm. (C) GAPDH–ferroportin FRET control, where instead of specific antibody against ferroportin, control goat IgG was utilized for donor staining. The acceptor is same as in Fig. 6B. Scale bars: 10 μm. (D) FRET efficiency (calculated as described in for Fig. 3C) as compared to that of nonspecific control (instead of goat anti-ferroportin antibody normal goat IgG was utilized); $P<0.0001$; $n=15$ cells. (E) Co-immunoprecipitation (Co-IP) of ferroportin and GAPDH from the cell surface of iron-loaded J774 cells. The membrane fraction was prepared from iron-treated J774 cells (2×10^7 cells) and immunoprecipitated using mouse monoclonal anti-GAPDH immobilized on anti-mouse-IgG−Magnabeads. Interaction with ferroportin was confirmed by western blotting with goat anti-ferroportin antibody. A negative (-ve) control was run in parallel, wherein the membrane fraction was co-immunoprecipitated using isotype control mouse IgG immobilized on anti-mouse-IgG–Magnabeads, whereas the membrane fraction of iron-loaded J774 cells served as positive control for ferroportin. (F) Higher-order multifunctionality of GAPDH – a model for its role in cellular iron efflux.

apotransferrin onto the cell surface, thereby increasing its local concentration in close proximity to ferroportin, so that iron exported through ferroportin is rapidly chelated. This is crucial, as localized high concentrations of free iron around the cell membrane can cause lipid peroxidation and compromise membrane integrity. Studies in *Xenopus* oocytes (which express ferroportin) have demonstrated the requirement of apotransferrin for increased iron efflux (Donovan et al., 2000). The increase in cell surface GAPDH upon iron overload, observed by us, also matches with the previously reported alterations in ferroportin expression in different cell types. Upon iron loading, ferroportin expression is decreased on the basolateral surface of enterocytes so as to decrease iron entry into the systemic circulation (Thomas and Oates, 2004). By contrast, ferroportin expression is increased on the surface of macrophages and hepatocytes to facilitate iron export out of these cells for maintaining homeostasis (Delaby et al., 2005; Ramey et al., 2010). In accordance with these reports, we have observed a decreased surface GAPDH expression, decrease in apotransferrin binding and a marginal effect on iron export in iron-loaded enterocytes upon incubation with apotransferrin, whereas control untreated enterocytes displayed a significant increase in iron export when incubated with apotransferrin. This can be explained by the fact that enterocytes are involved in dietary iron absorption and they export iron absorbed from the gut lumen into systemic circulation, thus making it available to the whole organism. In presence of excess iron, they would seek to minimize their iron export into the plasma so as to restrict the addition of more iron into the circulation. Macrophages and

hepatocytes demonstrated increased surface GAPDH and apotransferrin binding upon iron overload (as has been reported for ferroportin) to maintain iron homeostasis. Our *in vivo* studies in iron-loaded rats validated our results from cell culture experiments. We found an increase in surface GAPDH expression and apotransferrin binding in hepatocytes and peritoneal macrophages, whereas both decrease in the case of enterocytes as compared with cells isolated from control rats.

GAPDH is a protein with a diverse range of functions (Sirover, 2011; Sirover, 2012). Previous investigations revealed an additional role for GAPDH as a receptor for the trafficking of holotransferrin into iron-starved cells. Here, we demonstrate that, by changing the isoform recruited to the membrane, GAPDH additionally functions as a high-affinity receptor for apotransferrin, thereby maintaining iron homeostasis by enhancing cellular iron egress. Our current studies uncover an additional order of multifunctionality for GAPDH (multifunctionality within multifunctionality), wherein it switches its role under the diametrically opposite conditions of cellular iron status, providing a two-way switch based on the modification of PTMs for cellular iron regulation. In addition, to the best of our knowledge this is also the first report that clearly identifies a high-affinity apotransferrin receptor and provides a clear mechanism for its role in managing cellular iron. A schematic model of this dual role of GAPDH is outlined in Fig. 7F.

MATERIALS AND METHODS

Cell lines, primary cells and materials

All cell lines (including a stable THP1 cell line in which knockdown of total cellular GAPDH had been previously established), primary cells (Sprague Dawley rat peritoneal and spleen macrophages, enterocytes and hepatocytes) were obtained, purified and maintained essentially as described previously (Sheokand et al., 2013). THP1 cells were activated for 24 hours with 12.5 ng/ml of phorbol 12-myristate 13-acetate (PMA). All cells were maintained in RPMI-1640 medium supplemented with 10% fetal calf serum.

Purified RBCs were labeled by using the CellVue® Claret Far Red Florescent Cell Linker Midi Kit (Sigma) as per the manufacturer's instructions. Rabbit anti-RBC serum was raised and validated using standard methods. Erythrocytes were opsonized by incubation with antisera (1:50 dilution) at 37℃ for 1 hour followed by three washes with PBS. Animal experiments and the collection of blood from healthy volunteers was performed with due approval from the relevant institutional ethical committees.

Cell treatments

The iron concentration of cells was increased by culturing cells in medium containing 100 µM $FeCl_3$ as described previously (Foster et al., 2001). Excess iron was thus presented as ferrous ascorbate to increase solubility and facilitate cellular accumulation (Han et al., 1995). Iron in macrophage cells was also enhanced by erythrophagocytosis (EPG), which was performed by incubating a monolayer of macrophages with opsonized RBCs (50:1) for 24 hours in complete medium (Knutson et al., 2005). Controls were set up in parallel with normal medium. Extracellular RBCs were lysed with distilled water for 2 minutes, followed by rinsing cells with neutral buffer (20 mM HEPES, 150 mM NaCl, 5 mM KCl and 1 mM each of $CaCl_2$ and $MgCl_2$). For *in vivo* acute iron loading, Sprague Dawley rats were injected intraperitoneally with 100 mg iron dextran (Sigma) or 1×10^9 opsonized RBCs and, after 24 hours, peritoneal macrophages were isolated as described previously (Sheokand et al., 2013). For iron depletion experiments, cells were cultured in complete medium with 100 µM desferrioxamine (DFO) as described previously (Kumar et al., 2012). No significant change in cell viability due to any treatment was observed, as assessed by several independent viability assays described previously (Kumar et al., 2012; Sheokand et al., 2013). In addition, a Caspase-Glo™ 3/7 assay kit (Promega) was also utilized to confirm the absence of any induction of cell apoptosis.

Protein conjugates

Rabbit muscle GAPDH was obtained from Sigma, and apotransferrin was procured from Calbiochem. Proteins were conjugated to flurochromes or biotin by standard procedures using FITC (Sigma), Hilyte Fluor 647 protein labeling kit (Anaspec) and sulfo-NHS-LC biotin (Pierce).

Calcein quenching assay

Erythrophagocytosis was performed with a monolayer of macrophages as described above for cell treatments with controls set up in parallel with normal medium. Subsequently, cells were washed three times with serum-free medium (SFM) and incubated with 500 nM Calcein AM at 37℃ for 10 minutes. After extensive washing with SFM, the fluorescence of intracellular dye was measured by flow cytometry. As Calcein fluorescence is quenched by iron, a decrease in cellular fluorescence is indicative of an increased intracellular labile iron pool.

Enzyme activity of cell surface GAPDH and flow cytometry analysis

Ectoenzyme activity analysis of intact control or $FeCl_3$-treated J774 cells was performed essentially as described previously (Raje et al., 2007). All flow cytometry experiments were performed as described previously (Raje et al., 2007). Briefly, 2×10^5 cells/tube were stained with 1 µg of anti-GAPDH antibody (Calbiochem) or isotype control (mouse IgG), followed by sheep anti-mouse-IgG–FITC $(Fab)_2$ (Sigma), or with anti TfR1–PE or isotype control (BD), with 10 µg of holotransferrin–Alexa-Fluor-647 or with apotransferrin–Alexa-Fluor-647. For apotransferrin staining, 100 µM DFO was included in the incubation buffer so as to prevent conversion of the apo form of transferrin to holotransferrin. For intracellular GAPDH staining, cells were fixed with 1% paraformaldehyde and permeablized using 0.1% saponin at 37℃ for 15 minutes before staining. Analysis of 10^4 cells was performed for each sample using the FACS Calibur or FACS Verse flow cytometer (BD).

Flow cytometric differential detergent-resistant ratio of GAPDH

Control or iron-loaded J774 cells were analyzed for the FCDR ratio of surface GAPDH exactly as described previously (Kumar et al., 2012).

2D analysis of membrane-associated GAPDH

J774 cells were treated with DFO or excess iron, and membrane fractions were prepared essentially as described previously (Raje et al., 2007). Membrane proteins (200 µg from either DFO- or $FeCl_3$-treated J774 cells) were purified by using the Biorad Protein Cleanup Kit® as per the manufacturer's instructions and were subsequently dissolved in solubilization buffer (2 M thiourea, 7 M urea, 3% CHAPS, 20 mM Tris) to a final volume of 125 µl. IPG 7 cm, pH 3–10 linear gradient strips (BioRad) were loaded with samples by rehydration-loading. Isoelectric focusing was performed at 0–250 V for 2 hours (linear), 250 V for 1 hour (rapid) and 250 V–3000 V for 4 hours (linear), then 3000 V was maintained until 15,000 V-hours was achieved. The current was limited to 50 µA per strip, and the temperature was kept at 20℃ for all isoelectric focusing steps. For the second dimension SDS-PAGE, the IPG strips were incubated in equilibration buffer 1 (6 M urea, 2% SDS, 20% glycerol, 0.375 M Tris-HCl pH 8.8, 2% DTT) for 10 minutes, followed by incubation in equilibration buffer 2 (6 M urea, 2% SDS, 20% glycerol, 0.375 M Tris-HCl pH 8.8, 2.5% iodoacetamide) for another 10 minutes and then transferred onto 4–15% gradient acrylamide gels (Biorad). The gels were run at 25 mA until the Bromophenol Blue front had reached the bottom of the gel. Resolved proteins were processed for western blotting and immunodetection of GAPDH as described previously (Raje et al., 2007).

LC-MS/MS analysis of membrane-associated GAPDH from iron-depleted and iron-treated cells

J774 cells were treated with DFO or excess iron, and membrane fractions were prepared as described above. Extracted membrane proteins (200 µg from either DFO- or $FeCl_3$-treated J774 cells) were subjected to SDS-PAGE and stained with Coomassie Brilliant Blue. Bands corresponding to GAPDH were excised and destained with 200 mM of NH_4HCO_3 in 40% acetonitrile

(ACN) at 37℃ for 30 minutes. Subsequently, gel pieces were dried in a Speed Vac® and incubated at 37℃ in digestion buffer containing 20 ng/µl trypsin (Sigma) and 40 mM NH_4HCO_3 in 9% ACN for 18 hours. Finally, supernatant was collected for digested peptides and subjected to LC-MS/MS analysis. Peptides were analyzed by ultra-high-performance liquid chromatography (UPLC)/ESI/MS/MS with mass spectrometer (Q-TOF 6550, Agilent). Peptides were separated using a C_4 reversed-phase, 3.5-µm, 2.1×150-mm analytical column (X Bridge™ BEH 300, Waters). A sample volume of 8 µl was injected, and the flow rate was maintained at 400 µl/min. The mobile phase constituted 90% solution A (0.1% formic acid, 90% water, 10% ACN) and 10% of solution B (0.1% formic acid, 90% ACN, 10% water) for 15 minutes, 70% solution A:30% solution B for 8 minutes, 40% solution A:60% solution B for 5 minutes, 10% solution A:90% solution B for 2 minutes, 50% solution A:50% solution B for 2 minutes and 90% solution A:10% solution B for 2 minutes over a time period of 32 minutes. The capillary voltage was 1.5 kV, and a dry gas flow rate of 13 l/min was used, with a temperature of 220℃. The scan range used was 100–3200 m/z. The tandem mass spectra were annotated and peak list files (.MGF) were generated. Data analysis was performed essentially as described previously (Seo et al., 2008). Protein identification was performed by searching in the National Center for Biotechnology Information non-redundant database (NCBInR) using the Mascot program (Matrix Science) with the following parameters: peptide mass tolerance, 1.2 Da; MS/MS ion tolerance, 0.6 Da; taxonomy was limited to *Mus musculus*; allow up to one missed trypsin cleavage site; variable modifications considered were: acetylation (K), deamidation (N, Q), methylation (D, E), dimethylation (N, R, K), oxidation (M, C), phosphorylation (S, T, Y), cysteine propionamide, conversion of proline to pyroglutamic acid (pyro-Glu; P), pyro-Glu (N-terminal, E, Q), nitrosylation (C), succinylation (K), ADP-ribosylation (K), palmitoylation (C), myristoylation (N-terminal, G), farnesylation (C) and GPI anchor (protein C-terminal). Only significant hits as defined by Mascot probability analysis were considered. In addition, a minimum total score of 50, comprising at least one peptide match of ion score >20 was arbitrarily set as the threshold for acceptance (Seo et al., 2008).

In vitro interaction of GAPDH–apotransferrin by solid-phase assays

In vitro interaction of GAPDH and apotransferrin was analyzed by ELISA and surface plasmon resonance (SPR)-based affinity interaction analysis by standard procedures as described previously (Raje et al., 2007). Briefly, polystyrene ELISA plate wells were coated overnight at 4℃ using 150 nM/well of rabbit muscle GAPDH in PBS and blocked with 5% bovine serum albumin (BSA) for 24 hours at 4℃. Wells were then incubated with different concentrations of apotransferrin in PBST (PBS+0.05% Tween-20) containing 0.5% BSA for 24 hours at 4℃. After extensive washing, the bound apotransferrin was detected by incubation with rabbit anti-transferrin antibody followed by goat anti-rabbit-IgG–HRP. TMB H_2O_2 substrate for ELISA (Bangalore Genei) was used to develop the reaction and the optical density (OD) was measured at 450 nm. As a positive control for apotransferrin, a set of wells were coated with apotransferrin alone. Controls were also set up to determine the nonspecific interaction of; (i) anti-transferrin antibody with GAPDH, (ii) anti-transferrin antibody with BSA, (iii) transferrin with BSA, (iv) secondary antibody with GAPDH and (v) secondary antibody with BSA. Each set consisted of four wells in replicates. For the SPR assay, biotinylated apotransferrin was immobilized on sensor chip SA (Biacore) as per the manufacturer's instructions (Biacore 3000). Subsequently, increasing concentrations of GAPDH were used as an analyte in HBS-EP buffer (Biacore) at pH 7.4. Regeneration of the sensor chip was performed using 250 mM NaOH. K_{on}, K_{off} and K_D values were determined by using 1:1 binding model Biacore 3000® evaluation software (Raje et al., 2007).

Apotransferrin binding to iron-loaded cells is pronase sensitive and specific

Excess-iron-treated J774 cells were pretreated with 0.1% pronase (Roche) or control buffer for 20 minutes at 4℃. Subsequently, cells were washed with SFM and stained with apotransferrin–Alexa-Fluor-647 at 4℃ for 1 hour. Nonspecific binding was evaluated by incorporating 200× unlabeled apotransferrin in the staining mixture. All samples were analyzed by flow cytometry.

Binding of apotransferrin to cells is saturable

The characteristics of apotransferrin binding to cells were assessed essentially as described previously (Kumar et al., 2012). Briefly, J774 cells were cultured in 96-well plates (2×10^4 cells/well) and loaded with iron by incubation with 100 µM $FeCl_3$ for 24 hours. Subsequently, cells were incubated with increasing concentrations of biotinylated apotransferrin, either alone or in the presence of 200× unlabeled apotransferrin (to evaluate nonspecific interactions) for 2 hours at 4℃. This was followed by incubation with streptavidin–HRP (diluted 1:5000) for 45 minutes at 4℃. The reaction was developed with TMB H_2O_2. To determine the binding affinity, apotransferrin concentration versus OD data was fitted by nonlinear regression for one site total saturable binding using GraphPad® software.

Colocalization of cell surface proteins by confocal microscopy

Excess-iron-treated J774 cells were washed and blocked with neutral buffer containing 5% each of FCS and normal human serum. For cell surface colocalization of GAPDH and apotransferrin, cells were incubated with 1 µg of monoclonal anti-GAPDH (Calbiochem), followed by rabbit anti-mouse-IgG–Alexa-Fluor-568 (Molecular Probes) and 10 µg of apotransferrin–FITC. For simultaneous colocalization of GAPDH, apotransferrin and ferroportin, goat anti-ferroportin antibody (diluted 1:100; Santa Cruz Biotechnology) was included in the above antibody incubation mixture. After extensive washing, cells were incubated with rabbit anti-mouse-IgG–Alexa-Fluor-568 (for the detection of GAPDH), followed by mouse anti-goat-IgG–FITC (Santa Cruz Biotechnology) and 10 µg of apotransferrin–Alexa-Fluor-647. All antibody incubations were carried out sequentially at 4℃. Finally, cells were washed, fixed in 1% paraformaldehyde and imaged with a confocal microscope (Nikon A1R), using a 63× oil-immersion objective and 1 Airy unit aperture as described previously (Sheokand et al., 2013). The colocalization of signals was visualized manually in the merged image, and Pearson's correlation coefficient was calculated using Nikon NIS-Elements® software.

Interaction of GAPDH–apotransferrin and GAPDH–ferroportin

The interaction of proteins on the surface of iron-loaded J774 cells was assessed by confocal-microscopy-based colocalization, co-immunoprecipitation and acceptor-photobleaching FRET analysis as described previously (Raje et al., 2007; Sheokand et al., 2013). For co-immunoprecipitation of GAPDH and apotransferrin, 2×10^7 iron-treated J774 cells were incubated with 500 µg of biotinylated apotransferrin in 1 ml of FACS buffer for 1 hour on ice. Controls were set up in parallel, wherein the incubation of cells with biotinylated apotransferrin was omitted. Cells were washed and processed for preparation of the membrane protein fractions. Co-immunoprecipitation was performed from these fractions using streptavidin–Magnabeads® (Polysciences) as per the manufacturer's instructions. The beads were boiled in SDS sample buffer, and eluted proteins were analyzed by western blotting using a monoclonal anti-GAPDH antibody. For co-immunoprecipitation of GAPDH and ferroportin, iron-treated J774 cells were processed for preparation of the membrane protein fraction as described above. Co-immunoprecipitation was performed using monoclonal anti-GAPDH immobilized onto anti-mouse-IgG–Magnabeads® (Polysciences). A negative control was performed in parallel, wherein the membrane fraction was co-immunoprecipitated using isotype control mouse IgG immobilized on anti-mouse-IgG–Magnabeads. The beads were boiled in SDS sample buffer, and eluted proteins were analyzed by western blotting using an anti-ferroportin antibody.

In vivo study in a rodent model

Male Sprague-Dawley rats (150–170 g) of 4–6 weeks of age were administered with a total of 700 mg of iron dextran intraperitoneally over a 16-week period essentially as described previously (Brown et al., 2007). These procedures were approved by the institutional animal ethics committee. Groups of animals were sacrificed over a period of 1 week.

Hepatocytes, peritoneal macrophages and enterocytes were isolated and stained for surface GAPDH and apotransferrin, and analyzed by flow cytometry. Liver tissue and serum samples were assayed for iron using the Quantichrome iron assay kit.

Chromogenic iron-release assay

J774 cells were treated with 100 µM $FeCl_3$ for 24 hours and harvested. Aliquots of 1×10^6 cells were incubated with 100 µl of SFM or SFM supplemented with 0.3 mg apotransferrin at 37℃ for 1 hour. Subsequently, cells were centrifuged (500 ***g***, 5 minutes) to collect supernatant. The cell pellet was washed three times with neutral buffer (20 mM HEPES, 150 mM NaCl, 5 mM KCl and 1 mM each of $CaCl_2$ and $MgCl_2$). Both the cell pellet and the respective cell supernatant were digested with 5% HNO_3 at 80℃ for 2 hours to release iron. Samples were concentrated in a Speed Vac concentrator, and iron estimation was performed using a Quantichrome® iron assay kit (Bioassay systems) as per the manufacturer's instructions.

Iron-release assay using radioactive iron

Cells were loaded with iron either by incubation with $FeCl_3$ or by erythrophagocytosis (spleen macrophages, THP1 and J774) in complete medium spiked with 500 nM of $^{55}FeCl_3$ (ARC) at 37℃. Controls were set up in parallel with complete medium containing 500 nM of $^{55}FeCl_3$. After 12 hours, cells were washed extensively with SFM and incubated with 200 µl of SFM containing 2 mg/ml apotransferrin or with only SFM (as a control). Subsequently, the cell-free supernatants were collected and assayed for the presence of ^{55}Fe by liquid scintillation counting.

Sequestration of exported iron by apotransferrin

J774 cells cultured in 24-well plates (3×10^5 cells/well) were iron loaded by $FeCl_3$ treatment along with 500 nM $^{55}FeCl_3$ as for the iron-release assays described above. Cells were then incubated with 0.5 mg/ml biotinylated apotransferrin at 37℃ for 1 hour in SFM. Subsequently, the supernatant was collected and biotinylated apotransferrin was captured using streptavidin–Magnabeads. Precipitated samples were blotted onto nitrocellulose membrane and radioactive iron was detected using a phosphoimager (Fujifilm FLA-9000).

Statistical analysis

All statistical analysis was performed using unpaired Student's *t*-test.

Acknowledgements

Anil Theophilus and Subash Pawar (Institute of Microbial Technology, Chandigarh, India) are acknowledged for technical assistance. This is IMTECH communication number 0140/2013.

Competing interests

The authors declare no competing interests.

Author contributions

M.R. and C.I.R. conceived the study. M.R., C.I.R., N.S. and H.M. designed the experiments and analyzed the data. N.S., H.M., V.A.T. and A.S.C. contributed to the *in vivo* rodent study and 2D gel electrophoresis experiments. N.S. and S.K. contributed to *in vivo* affinity experiments. M.R., C.I.R. and N.S. wrote the manuscript.

Funding

N.S., H.M. and A.S.C. received fellowships from the Council for Scientific and Industrial Research (CSIR), University Grants Commission and Department of Biotechnology, respectively. The financial support of CSIR and the Department of Science and Technology is acknowledged.

Supplementary material

Supplementary material available online at
http://jcs.biologists.org/lookup/suppl/doi:10.1242/jcs.154005/-/DC1

References

Abboud, S. and Haile, D. J. (2000). A novel mammalian iron-regulated protein involved in intracellular iron metabolism. *J. Biol. Chem.* **275**, 19906-19912.

Andrews, N. C. (2000). Iron homeostasis: insights from genetics and animal models. *Nat. Rev. Genet.* **1**, 208-217.

Auriac, A., Willemetz, A. and Canonne-Hergaux, F. (2010). Lipid raft-dependent endocytosis: a new route for hepcidin-mediated regulation of ferroportin in macrophages. *Haematologica* **95**, 1269-1277.

Bergamaschi, G., Eng, M. J., Huebers, H. A. and Finch, C. A. (1986). The effect of transferrin saturation on internal iron exchange. *Proc. Soc. Exp. Biol. Med.* **183**, 66-73.

Brown, K. E., Broadhurst, K. A., Mathahs, M. M. and Weydert, J. (2007). Differential expression of stress-inducible proteins in chronic hepatic iron overload. *Toxicol. Appl. Pharmacol.* **223**, 180-186.

Burke, W., Imperatore, G. and Reyes, M. (2001). Iron deficiency and iron overload: effects of diet and genes. *Proc. Nutr. Soc.* **60**, 73-80.

Canonne-Hergaux, F., Donovan, A., Delaby, C., Wang, H. J. and Gros, P. (2006). Comparative studies of duodenal and macrophage ferroportin proteins. *Am. J. Physiol.* **290**, G156-G163.

Casey, J. L., Hentze, M. W., Koeller, D. M., Caughman, S. W., Rouault, T. A., Klausner, R. D. and Harford, J. B. (1988). Iron-responsive elements: regulatory RNA sequences that control mRNA levels and translation. *Science* **240**, 924-928.

Choudhary, S., De, B. P. and Banerjee, A. K. (2000). Specific phosphorylated forms of glyceraldehyde 3-phosphate dehydrogenase associate with human parainfluenza virus type 3 and inhibit viral transcription in vitro. *J. Virol.* **74**, 3634-3641.

Delaby, C., Pilard, N., Gonçalves, A. S., Beaumont, C. and Canonne-Hergaux, F. (2005). Presence of the iron exporter ferroportin at the plasma membrane of macrophages is enhanced by iron loading and down-regulated by hepcidin. *Blood* **106**, 3979-3984.

Donovan, A., Brownlie, A., Zhou, Y., Shepard, J., Pratt, S. J., Moynihan, J., Paw, B. H., Drejer, A., Barut, B., Zapata, A. et al. (2000). Positional cloning of zebrafish ferroportin1 identifies a conserved vertebrate iron exporter. *Nature* **403**, 776-781.

Dunn, L. L., Suryo Rahmanto, Y. and Richardson, D. R. (2007). Iron uptake and metabolism in the new millennium. *Trends Cell Biol.* **17**, 93-100.

Fleming, R. E. and Ponka, P. (2012). Iron overload in human disease. *N. Engl. J. Med.* **366**, 348-359.

Foster, S. L., Richardson, S. H. and Failla, M. L. (2001). Elevated iron status increases bacterial invasion and survival and alters cytokine/chemokine mRNA expression in Caco-2 human intestinal cells. *J. Nutr.* **131**, 1452-1458.

Ganz, T. (2007). Molecular control of iron transport. *Journal of the American Society of Nephrology: JASN* **18**, 394-400.

Ganz, T. (2013). Systemic iron homeostasis. *Physiol. Rev.* **93**, 1721-1741.

Glaser, P. E. and Gross, R. W. (1995). Rapid plasmenylethanolamine-selective fusion of membrane bilayers catalyzed by an isoform of glyceraldehyde-3-phosphate dehydrogenase: discrimination between glycolytic and fusogenic roles of individual isoforms. *Biochemistry* **34**, 12193-12203.

Gombos, I., Bacsó, Z., Detre, C., Nagy, H., Goda, K., Andrásfalvy, M., Szabó, G. and Matkó, J. (2004). Cholesterol sensitivity of detergent resistance: a rapid flow cytometric test for detecting constitutive or induced raft association of membrane proteins. *Cytometry* **61A**, 117-126.

Grillon, J. M., Johnson, K. R., Kotlo, K. and Danziger, R. S. (2012). Non-histone lysine acetylated proteins in heart failure. *Biochim. Biophys. Acta* **1822**, 607-614.

Han, O., Failla, M. L., Hill, A. D., Morris, E. R. and Smith, J. C., Jr (1995). Ascorbate offsets the inhibitory effect of inositol phosphates on iron uptake and transport by Caco-2 cells. *Proc. Soc. Exp. Biol. Med.* **210**, 50-56.

Hentze, M. W., Muckenthaler, M. U. and Andrews, N. C. (2004). Balancing acts: molecular control of mammalian iron metabolism. *Cell* **117**, 285-297.

Kawabata, H., Germain, R. S., Vuong, P. T., Nakamaki, T., Said, J. W. and Koeffler, H. P. (2000). Transferrin receptor 2-α supports cell growth both in iron-chelated cultured cells and in vivo. *J. Biol. Chem.* **275**, 16618-16625.

Knutson, M. and Wessling-Resnick, M. (2003). Iron metabolism in the reticuloendothelial system. *Crit. Rev. Biochem. Mol. Biol.* **38**, 61-88.

Knutson, M. D., Oukka, M., Koss, L. M., Aydemir, F. and Wessling-Resnick, M. (2005). Iron release from macrophages after erythrophagocytosis is up-regulated by ferroportin 1 overexpression and down-regulated by hepcidin. *Proc. Natl. Acad. Sci. USA* **102**, 1324-1328.

Kondo, H., Saito, K., Grasso, J. P. and Aisen, P. (1988). Iron metabolism in the erythrophagocytosing Kupffer cell. *Hepatology* **8**, 32-38.

Kong, W., Duan, X., Shi, Z. and Chang, Y. (2008). Iron metabolism in the mononuclear phagocyte system. *Progr. Nat. Sci.* **18**, 1197-1202.

Kumar, S., Sheokand, N., Mhadeshwar, M. A., Raje, C. I. and Raje, M. (2012). Characterization of glyceraldehyde-3-phosphate dehydrogenase as a novel transferrin receptor. *Int. J. Biochem. Cell Biol.* **44**, 189-199.

Kuyumcu-Martinez, N. M., Wang, G.-S. and Cooper, T. A. (2007). Increased steady-state levels of CUGBP1 in myotonic dystrophy 1 are due to PKC-mediated hyperphosphorylation. *Mol. Cell* **28**, 68-78.

Le Gac, G., Ka, C., Joubrel, R., Gourlaouen, I., Lehn, P., Mornon, J. P., Férec, C. and Callebaut, I. (2013). Structure-function analysis of the human ferroportin iron exporter (SLC40A1): effect of hemochromatosis type 4 disease mutations and identification of critical residues. *Hum. Mutat.* **34**, 1371-1380.

Lipschitz, D. A., Simon, M. O., Lynch, S. R., Dugard, J., Bothwell, T. H. and Charlton, R. W. (1971). Some factors affecting the release of iron from reticuloendothelial cells. *Br. J. Haematol.* **21**, 289-303.

Journal of Cell Science

Madian, A. G., Hindupur, J., Hulleman, J. D., Diaz-Maldonado, N., Mishra, V. R., Guigard, E., Kay, C. M., Rochet, J. C. and Regnier, F. E. (2012). Effect of single amino acid substitution on oxidative modifications of the Parkinson's disease-related protein, DJ-1. *Mol. Cell Proteomics* **11**, M111 010892.

McKie, A. T., Marciani, P., Rolfs, A., Brennan, K., Wehr, K., Barrow, D., Miret, S., Bomford, A., Peters, T. J., Farzaneh, F. et al. (2000). A novel duodenal iron-regulated transporter, IREG1, implicated in the basolateral transfer of iron to the circulation. *Mol. Cell* **5**, 299-309.

Modun, B., Evans, R. W., Joannou, C. L. and Williams, P. (1998). Receptor-mediated recognition and uptake of iron from human transferrin by Staphylococcus aureus and Staphylococcus epidermidis. *Infect. Immun.* **66**, 3591-3596.

Modun, B., Morrissey, J. and Williams, P. (2000). The staphylococcal transferrin receptor: a glycolytic enzyme with novel functions. *Trends Microbiol.* **8**, 231-237.

Nishisato, T. and Aisen, P. (1982). Uptake of transferrin by rat peritoneal macrophages. *Br. J. Haematol.* **52**, 631-640.

Park, K. S., Frost, B. F., Shin, S., Park, I. K., Kim, S. and Paik, W. K. (1988). Effect of enzymatic methylation of yeast iso-1-cytochrome c on its isoelectric point. *Arch. Biochem. Biophys.* **267**, 195-204.

Polati, R., Castagna, A., Bossi, A. M., Alberio, T., De Domenico, I., Kaplan, J., Timperio, A. M., Zolla, L., Gevi, F., D'Alessandro, A. et al. (2012). Murine macrophages response to iron. *J. Proteomics* **76**, 10-27.

Quail, E. A. and Yeoh, G. C. (1995). The effect of iron status on glyceraldehyde 3-phosphate dehydrogenase expression in rat liver. *FEBS Lett.* **359**, 126-128.

Raje, C. I., Kumar, S., Harle, A., Nanda, J. S. and Raje, M. (2007). The macrophage cell surface glyceraldehyde-3-phosphate dehydrogenase is a novel transferrin receptor. *J. Biol. Chem.* **282**, 3252-3261.

Rama, R., Sánchez, J. and Octave, J. N. (1988). Iron mobilization from cultured rat bone marrow macrophages. *Biochim. Biophys. Acta* **968**, 51-58.

Ramey, G., Deschemin, J. C., Durel, B., Canonne-Hergaux, F., Nicolas, G. and Vaulont, S. (2010). Hepcidin targets ferroportin for degradation in hepatocytes. *Haematologica* **95**, 501-504.

Rawat, P., Kumar, S., Sheokand, N., Raje, C. I. and Raje, M. (2012). The multifunctional glycolytic protein glyceraldehyde-3-phosphate dehydrogenase (GAPDH) is a novel macrophage lactoferrin receptor. *Biochem. Cell Biol.* **90**, 329-338.

Saito, K., Nishisato, T., Grasso, J. A. and Aisen, P. (1986). Interaction of transferrin with iron-loaded rat peritoneal macrophages. *Br. J. Haematol.* **62**, 275-286.

Sarkar, J., Seshadri, V., Tripoulas, N. A., Ketterer, M. E. and Fox, P. L. (2003). Role of ceruloplasmin in macrophage iron efflux during hypoxia. *J. Biol. Chem.* **278**, 44018-44024.

Seidler, N. W. (2013). *GAPDH: Biological Properties and Diversity*. Dordrecht; New York, NY: Springer.

Seo, J., Jeong, J., Kim, Y. M., Hwang, N., Paek, E. and Lee, K.-J. (2008). Strategy for comprehensive identification of post-translational modifications in cellular proteins, including low abundant modifications: application to glyceraldehyde-3-phosphate dehydrogenase. *J. Proteome Res.* **7**, 587-602.

Sheftel, A. D., Mason, A. B. and Ponka, P. (2012). The long history of iron in the Universe and in health and disease. *Biochim. Biophys. Acta* **1820**, 161-187.

Sheokand, N., Kumar, S., Malhotra, H., Tillu, V., Raje, C. I. and Raje, M. (2013). Secreted glyceraldehye-3-phosphate dehydrogenase is a multifunctional autocrine transferrin receptor for cellular iron acquisition. *Biochim. Biophys. Acta* **1830**, 3816-3827.

Siegenberg, D., Baynes, R. D., Bothwell, T. H., MacFarlane, B. J. and Lamparelli, R. D. (1990). Factors involved in the regulation of iron transport through reticuloendothelial cells. *Proc. Soc. Exp. Biol. Med.* **193**, 65-72.

Sirover, M. A. (2011). On the functional diversity of glyceraldehyde-3-phosphate dehydrogenase: biochemical mechanisms and regulatory control. *Biochim. Biophys. Acta* **1810**, 741-751.

Sirover, M. A. (2012). Subcellular dynamics of multifunctional protein regulation: mechanisms of GAPDH intracellular translocation. *J. Cell. Biochem.* **113**, 2193-2200.

Thomas, C. and Oates, P. S. (2004). Ferroportin/IREG-1/MTP-1/SLC40A1 modulates the uptake of iron at the apical membrane of enterocytes. *Gut* **53**, 44-49.

Umbreit, J. (2005). Iron deficiency: a concise review. *Am. J. Hematol.* **78**, 225-231.

Wessling-Resnick, M. (2006). Iron imports. III. Transfer of iron from the mucosa into circulation. *Am. J. Physiol.* **290**, G1-G6.

Xiu-Lian, D., Kui, W., Ya, K., Lan, Y., Rong-Chang, L., Yan Zhong, C., Kwok Ping, H. and Zhong Ming, Q. (2004). Apotransferrin is internalized and distributed in the same way as holotransferrin in K562 cells. *J. Cell. Physiol.* **201**, 45-54.

Zhang, H.-h., Wang, Y.-p. and Chen, D.-b. (2011). Analysis of nitroso-proteomes in normotensive and severe preeclamptic human placentas. *Biol. Reprod.* **84**, 966-975.